Proceedings World Geothermal Congress 2020+1
Reykjavik, Iceland, April - October 2021

Analysis of Performance and Reliability of BPPT 3MW Condensing Type Geothermal Power Plant – Kamojang during 3x24 hours Continuous Synchronous Testing

Bambang Teguh Prasetyo[1], Suyanto[2], Himawan Sutriyanto[1]

[1]Laboratory for Thermodynamics Engine and Propulsion Technology- BPPT, 230 Building, Puspiptek Area, Serpong - South Tangerang 15314, Indonesia.

[2]National Laboratory for Energy Conversion Technology, 620 Building, Puspiptek Area, Serpong - South Tangerang 15314, Indonesia

Email: bambang.teguh@bppt.go.id, suyanto.syt@gmail.com, himawan.sutriyanto@bppt.go.id

Keywords:geothermal power plant, small scale, condensing type, Kamojang, local content

ABSTRACT

BPPT has developed and operated a 3MW Geothermal Power Plant (GPP) of condensing type technology in Kamojang - Indonesia, which is the first prototype GPP manufactured by national companies. The GPP design is based on KMJ-68 well data characteristics, owned by Pertamina Geothermal Energy (PT. PGE), atmospheric conditions around the plant, and steam turbine specifications designed in reverse engineering. The manufacturing process of the main components of the plant such as turbines, generators, condensers, etc. carried out by the local manufacturer. This paper discusses the design of PFD, performance, and reliability of this plant during 3x24 hours continuous synchronous testing to the 20kV local power grid. Until the end of the testing in May 2019, the plant has produced 251MWh of electricity, with the highest load of 2.2 MW. During testing, the steam pressure and temperature entering the turbine are relatively constant around the design value. However, there is a loss of steam pressure entering the turbine by the strainer and reduced condenser vacuum which causes T/MWh from the plant to be relatively high. All process parameters, particularly vibrations, bearing temperatures, are all within the safe limit. This plant is very reliable in responding to local electricity network loads that often fluctuate. The thermal efficiency of the turbine generator is around 55%. This can still be improved by overcoming the problems of pressure loss in the filter and reducing condenser vacuum. The condenser vacuum can be optimized by keeping the cooling water temperature low. From the last inspection, a number of water spray nozzles in the cooling tower are clogged by dirt which is thought to be the cause of the increase in cooling water temperature. Thus it can be concluded that the plant is ready to operate with full load by increasing the performance of the cooling tower and strainer.

1. INTRODUCTION

Indonesia has the potential of abundant geothermal energy sources, with a total potential of more than 28 GW, from low to high enthalpy, which is spread along volcanic path from the islands of the Sumatra region, Java, Bali, NTT, Sulawesi to Maluku. Geothermal power plant (GPP) technology is one of the prospective renewable energy technologies and a priority in the development of national electricity today. Until the first quarter of 2018GPP installed capacity of 1,924 GW and all of them are imported technology. Therefore, effort to develop national GPP technology is very strategic to support national energy independence in the future. Referring to the direct steam plant working principle [1], Agency for the Assessment and Application of Technology (BPPT) has developed and operated a 3 MW GPP of condensing type technology in Kamojang - Indonesia, which is the first prototype GPP manufactured by local company.

The design of the GPP is based on the characteristic data of the KMJ-68 geothermal well owned by Pertamina Geothermal Energy, the atmospheric conditions around the plant, and the specifications of the steam turbine that has been reverse engineered. Some of the data used in design calculations refer to a number of literatures, such as in Table 1. Process Flow Diagrams (PFD) of the 3 MW GPP from the calculation of energy and mass balance are shown in Figure 1 and Table 2.

Table 1: Reference parameters for calculation of mass and energy balance

No.	Parameter	Value	Unit	References
1	Steam Pressure at well head	12	bara	Well test - KMJ-68, [2] and [3]
2	NCG content	1.7	%	Well test - KMJ-68, [2], [3] and [4]
3	Steam Pressure at inlet turbine	6.5	bara	Adjusted to turbine design
4	Turbine outlet pressure	0.16	bara	Adjusted to the condensation temperature (affected by environmental conditions), [2]
5	Cooling Water Temperature to Cooling Tower (CT)	45	˚C	Depending on the environmental conditions and CT design, [2]
6	Cooling water Temperature from CT	30	˚C	Depending on the environmental conditions, [2]
7	Turbine isentropic efficiency (η_t)	86 – 90	%	[5], [6], [7], [8]
8	Generator efficiency (η_{gen})	98.6 –98.7	%	[6], [9]
9	Mechanical efficiency (η_m)	98.6 – 99	%	[6]
10	Maximum Geo-fluid mass flowrate	30	tonne/hr	Well test - KMJ-68,[2]

The pressure of geo-fluid from the production well is reduced using restriction orifice (RO) to meet the turbine operating pressure. The steam is then separated from the solid particles and the dry steam inside the separator. Calculation of separator dimensions refers to requirements in [10, 11 and 12]. The steam out from the separator is then separated into three functions. First, the steam with the largest portion is used to drive the turbine. Second, the least steam portion, is used for the gland seal of the turbine after it taken into a lower pressure using RO. Third, with a large portion, is used as a motive steam in steam jet ejector (SJE) to attract non condensable gas (NCG) from inside the condenser. The NCG removal system (GRS) design refers to [3, 4, 13, 14, and 15], while the standards [16, 17, 18] are used in SJE design. In the turbine, the process of converting thermal energy into mechanical energy takes place to rotate the generator to produce electricity.

Exhaust steam from the turbine is condensed in the main condenser. Direct contact condenser is used in this installation. Thermal-fluid condenser calculations refer to [19], and for mechanical calculations refer to [20]. By using a hot-well pump, the condensate is pumped to the cooling tower (CT) to be cooled. Water from CT, mostly used as cooling media in the condenser which flows gravitationally. The rest is to cool the ejector condenser and the liquid ring vacuum pump (LRVP) with the help of the auxiliary cooling water pump (ACW). The excess water in CT is collected in the pond to be re-injected into the injection well. CT dimension calculations refer to standards [21].

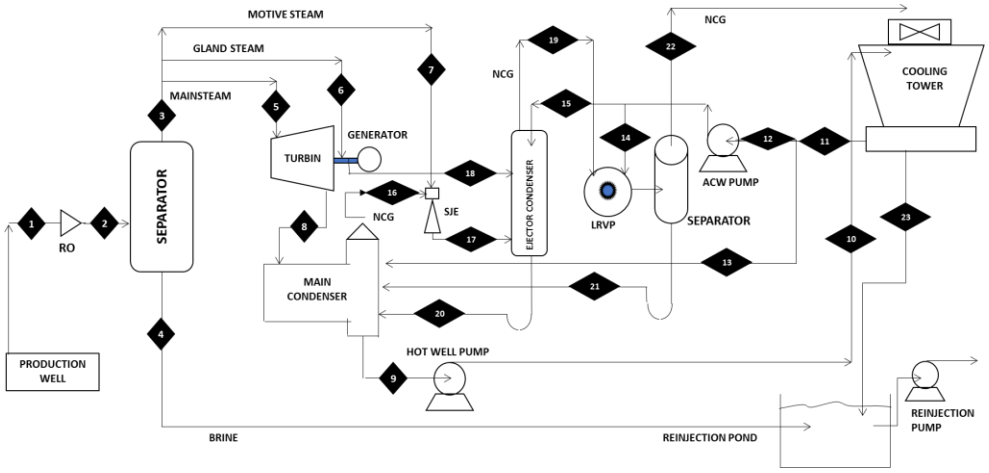

Figure 1: PFD Diagram of the BPPT's Small Scale 3 MW GPP Pilot Plant, Kamojang – West Java, Indonesia

Table 2: Process Parameters for each BPPT's 3MW GPP Components

Stream No.	1	2	3	4	5	6	7	8	9	10
Pressure (bara)	12	7	6.5	6.5	6.5	6.5	6.5	0.16	0.16	2.5
Temperature (°C)	188	165	165	162	162	162	162	55.3	49	49
SMF (kg/s)*)	8.316	8.316	8.233	0	7.622	0.038	0.573	6.667	0	0
NCG MF*) (kg/s)	0.141	0.141	0.140	0	0.13	0.001	0.001	0.001	0	0
WMF*) (kg/s)	0	0	0	0.083	0	0	0	0.955	226.33	226.33
AMFR*) (kg/s)	0	0	0	0	0	0	0	0		0

Stream No.	11	12	13	14	15	16	17	18	19	20
Pressure (bara)	1	1	1	1	1	0.16	0.4	1	0.4	0.16
Temperature (°C)	30	30	30	30	30	49	55.3	99.6	35	35
SMFR (kg/s)*)	0	0	0	0	0	0.021	0.594	0.038	0	0
NCG MFR*) (kg/s)	0	0	0	0	0	0.130	0.139	0.00065	0.139	0
WMFR*) (kg/s)	219.07	69.373	149.7	0.303	69.07	0	0	0	0	69.664
AMFR*) (kg/s)		0	0	0	0	0	0.004	0.004	0	0.004

Stream No.	21	22	23
Pressure (bara)	1	1	1
Temperature (°C)	30	35	30
SMFR (kg/s)*)	0	0	0
NCG MFR*) (kg/s)	0	0.139	0
WMFR*) (kg/s)	0.303	0	7.261
AMFR* (kg/s)	0	0.004	0

NOTE: *)
SMFR = Steam Mass Flow Rate, NCG MF =NCG Mass Flow Rate, WMFR = Water Mass Flow Rate, AMFR =Air Mass Flow Rate

Fabrication of the main components of the GPP such as turbine, generator, condensers, etc. is carried out by local industries. The integration of the main equipment of the turbine-generator is shown in Figure 2

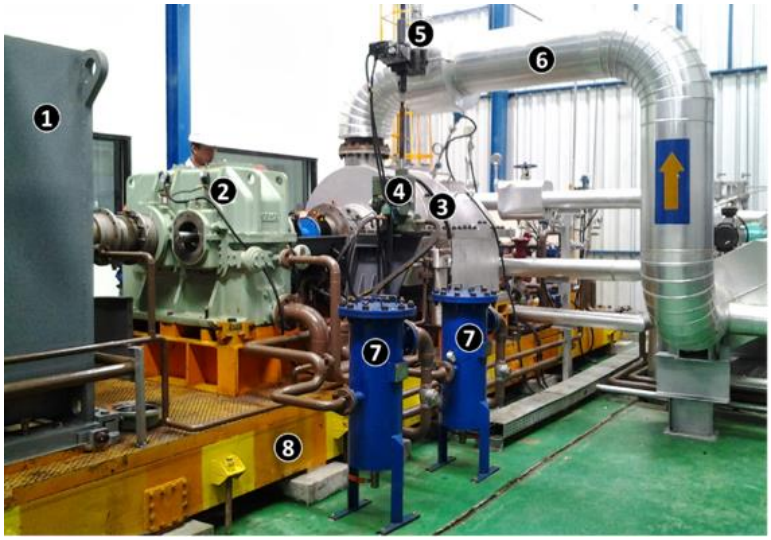

Figure 2: Installation of 3MW GPP, Kamojang, Indonesia

2. TESTING METHODOLOGY

2.1 Refer to previous synchronous test

For testing activities, a Standard Operating Procedure (SOP) for plant operations has been prepared. In the SOP, each activity is regulated starting from test preparation, plant start-up, no-load test, synchronous test, plant shutdown and plant emergency system. Synchronous initial testing has been carried out several times with the highest load of 1.8MW. Detailed explanations regarding test preparation and the results of previous synchronous tests can be seen in [25]. The last synchronous test was carried out on March 13-16 2019. The results show that the plant performance is quite good with thermal efficiency close to its design value. The resulting vibration is still below the maximum allowable value, and there is a downward trend for higher load. Similarly, the maximum value of the bearing temperature is still lower than the maximum allowable value. Thus, it can be concluded that 3MW GPP is feasible to proceed for operations at higher loads.

2.2 Synchronous Testing 3x24 hours(May7-10, 2019) to the 20kV Electricity Grid of PLN Garut-5 Region

Referring to the procedures, settings and results of previous synchronous tests [25], 3x24 hour synchronous testing has been carried out at higher loads on 7-10 May 2019. Electricity generated by the 3 MW GPP is channeled to a 20kV grid owned by the PLN network in Garut-5 region. In this testing period, the plant has actually been synchronized to the network since 7 May 2019 at 21.01 Western Indonesia Time (WIB) to a load of 1.9 MW. However, on May 8, 2019 at 3:37 a.m. WIB suddenly the plant was tripped. From the data acquisition system monitoring screen, no data anomalies were found. However, from the search of data records, it was found that the tripping command came from the HH sensor anomaly in the condenser. After repairing the sensor, the plant can be synchronized again on May 8, 2019 at 17.34 WIB until it reaches the highest load of around 2.2 MW. Therefore, in this paper, observations of the test results are presented only for 45 operating hours from May 8, 2019 at 17.34 Western Indonesia Time to May 10, 2019 at 14.12.30 WIB.

3. RESULTS AND DISCUSSION

For 45 operation hours of synchronous testing to the electricity network, all operating data is recorded in the data acquisition system. In this paper, observations are focused on pressure, temperature and mass flow rate of steam before strainer ($\mathbf{P_i}$, $\mathbf{T_i}$ and $\mathbf{F_i}$), pressure of steam after strainer at turbine inlet ($\mathbf{P_{ias}}$), pressure loss in the steam strainer ($\mathbf{dP_S}$), turbine-generator rotational speed and electrical power output (**RPM** and **Power**), condenser vacuum and temperature ($\mathbf{P_o}$ and $\mathbf{T_o}$), system vibration and bearing temperature.

Figure 3 shows $\mathbf{P_i}$, $\mathbf{P_{ias}}$ and $\mathbf{T_i}$ during 45 operation hours of synchronous test. $\mathbf{P_i}$ and $\mathbf{T_i}$ are relatively stable at around 6.4 bar and 176.5ºC, relatively close to the design (6.5bar and 162ºC). Fluctuations of $\mathbf{P_i}$ and $\mathbf{T_i}$ are around ±0.37% and ±0.11% respectively when the electric power has reached 1MW. There is a pressure loss in the steam strainer ($\mathbf{dP_S}$) indicated by the difference between $\mathbf{P_i}$ and $\mathbf{P_{ias}}$. $\mathbf{dP_S}$ gradually grew to reach around 0.57bar at the end of 3x24 hours of testing. This pressure loss will reduce the enthalpy of steam entering the turbine which causes the need for the steam flow rate to increase.

Figure 4 shows the RPM of the turbine and the electrical power produced by the plant. Turbine speed is relatively stable at 6490 rpm or about 0.075% above the design speed (6485 rpm). During synchronous testing, the governor operating mode is not base load but droop speed mode, it means that the plant load will fluctuate around the setting power following network frequency fluctuations. In figure 4, the plant's power fluctuates to 2.2MW while the setting power is around 1.85MW.

Figure 5 shows the position of the vertical vibration measurement points. The vertical vibration measurements on turbine, gear box and generator bearings on the downstream and upstream sides of each are $\mathbf{T_{1V}}$, $\mathbf{T_{2V}}$, $\mathbf{GB_{1V}}$, $\mathbf{GB_{4V}}$, $\mathbf{G_{1V}}$ **and** $\mathbf{G_{2V}}$ as shown in Figure 6.Vibration observation of the turbine, gear box, and generator bearings show that all measurements are still below the allowable values of 4mm/s, 10mm/s, and 4mm/s respectively except $\mathbf{G_{2V}}$ which is always around 4,5mm/s and even increases to 5mm/s when the electric power reaches above 2.0MW. The same thing happened to the $\mathbf{G_{1V}}$ which increased more than 4mm/s, but still below 4.5mm/s, when the electric power reached 1.75MW. All vibrations tend to increase with the increasing electrical power, except for $\mathbf{GB_{1V}}$, $\mathbf{GB_{4V}}$. The pattern of the increasing vibration for each bearing at each increase in electrical power is similar except $\mathbf{G_{1V}}$ and

G_{2V} which have opposite patterns. The vibration spectrum analysis on the **G_{1V} and G_{2V}** indicates that the cause of high vibrations is unbalance in the rotor. However, the fact shows that vibrations are increased not because of an increase in rotation but by an increase in power so that vibrations may also be caused by structural rigidity in the form of shaft-bearing clearance that is too small. This fact is supported by data that the generator bearing temperature is relatively high compared to other bearing temperatures. The highest vibration in the turbine indicates the presence of misalignment in the turbine.

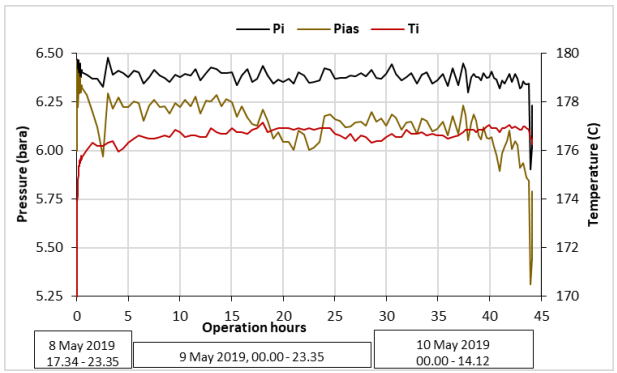

Figure 3: Steam turbine inlet pressure and temperature

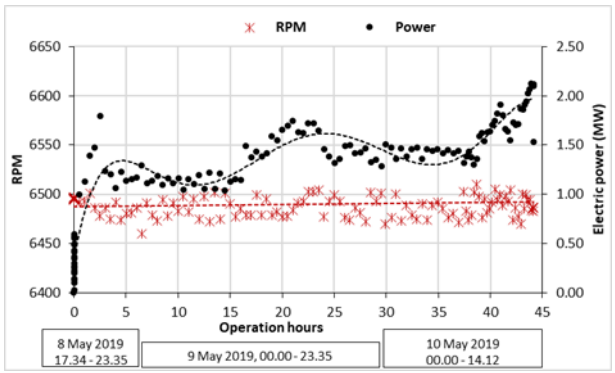

Figure 4: Turbine RPM and electric power

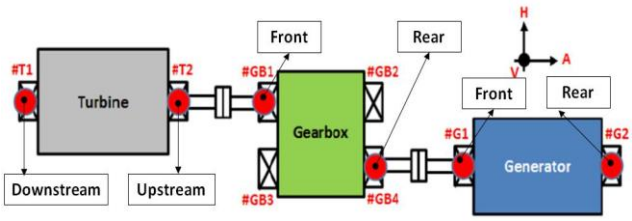

Figure 5: Vertical vibration measurement points

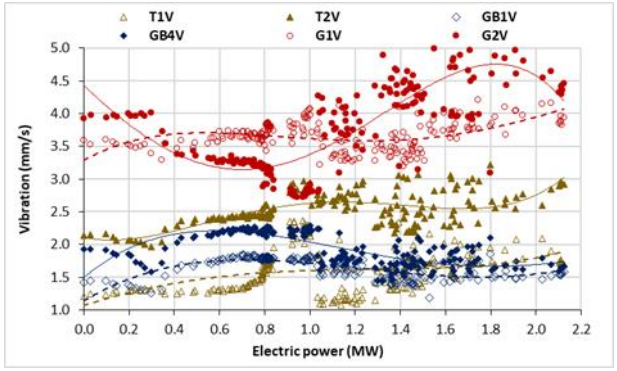

Figure 6: Vertical vibration vs Electric power

Figure 7 shows extreme temperatures on turbine and generator bearings. **TT_{001}** and **TT_{007}** are respectively the temperatures of the turbine journal bearings on the downstream and upstream sides. Whereas **TT_{003}** and **TT_{004}** are respectively turbine thrust bearing temperatures on the downstream side. As for **TT_{012}** and **TT_{013}**, each is a generator bearing temperature on the gearbox side and on the rear side. The four measurements of the temperature of the gearbox bearings are not displayed because the temperatures are

relatively normal, stable and low, around 45 - 50ºC. The tendency that occurs at the bearing temperature is, when the electric power is around 0 - 0.5MW all bearing temperatures are relatively stable at their respective values. The temperature of each bearing then increases significantly when the power increases from 0.5 to 1.25MW. Furthermore, at higher power, the temperature of each bearing will continue to increase even though it is relatively low. The temperature of the generator bearings (**TT_{012}** and **TT_{013}**) are relatively very high compared to the temperature of the other bearings on the turbine. The results of the study carried out together with the generator manufacturer have concluded that it may be caused by clearances between the shaft and the bearing that are too small. It is also rather strange that the temperature readings of one thermocouple on the thrust bearing (**TT_{003}**) are relatively high. For this, it may be due to the anomaly of the thermocouple installation on the bearing. Because on the other side of the same bearing, the temperature (**TT_{004}**) is relatively very low, around 45 - 50ºC. Besides that, the temperature of the bearing journal on the turbine both downstream and upstream (**TT_{001}** and **TT_{007}**) is also relatively normal and low, around 60ºC.

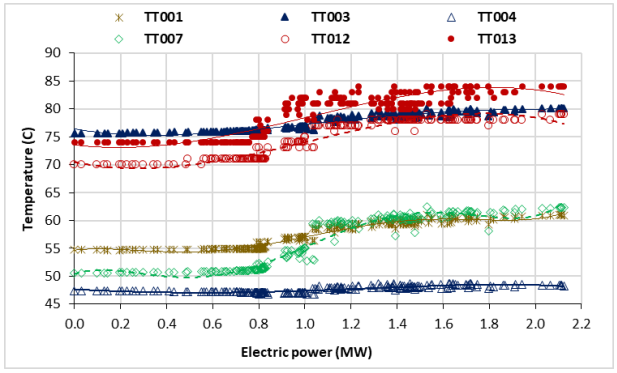

Figure 7: Bearings temperature vs Electric power

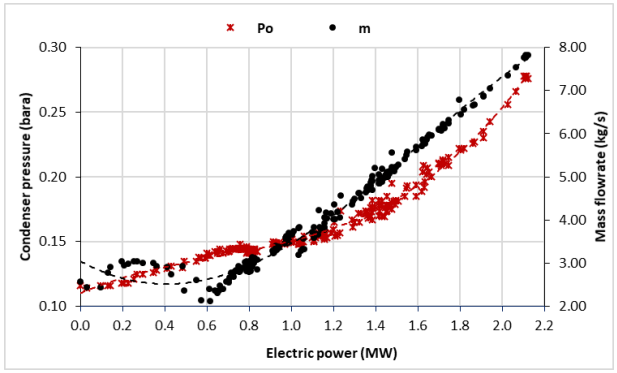

Figure 8: Condenser pressure and steam mass flowrate vs power

Figure 8 shows the mass flow rate of steam (**m**) and condenser pressure (**P_o**) as a function of electric power. At low power, steam consumption is relatively high even though the condenser vacuum is high. When electric power is higher than 0.6 MW, steam consumption increases significantly as power increases. This is because the condenser vacuum decreases significantly. From the test data, the condenser vacuum drop due to the condenser cooling water temperature from the cooling tower increases.

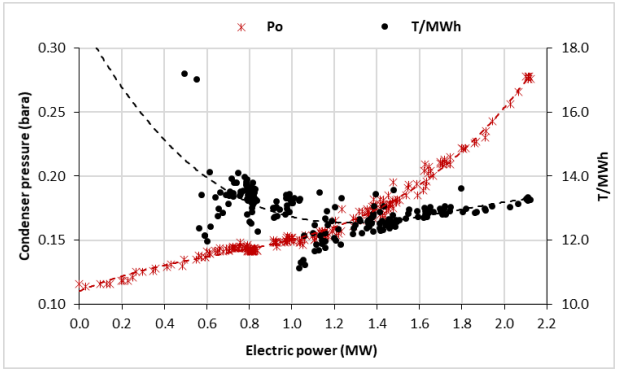

Figure 9: Condenser pressure and T/MWhvs Electric power

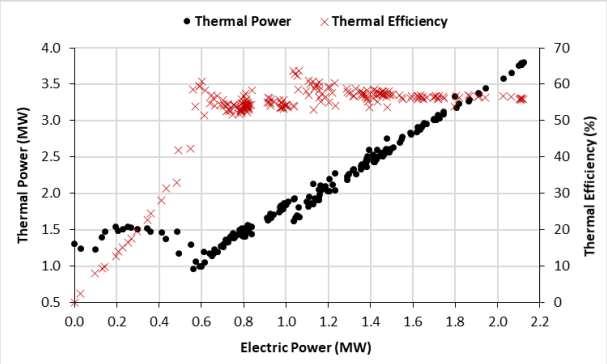

Figure 10: Thermal Power and Efficiency vs Electric power

One of the plant performance characteristics is expressed in the ratio of steam mass flow rates to electric power (T/MWh). Figure 9 shows T/MWh, condenser pressure and electric power. At low electrical power (<0.7MW), T/MWh is relatively high even though the condenser vacuum is high (<design value of 0,16bara). At a power between 0.7 - 1.25Mw, T/MWh decreases significantly when the vacuum condenser is relatively constant around the design value. At> 1.25MW, T / MWh increases slowly to 13T/MWh at a power of around 2.2MW. The possible cause of this phenomenon is that the condenser vacuum gradually decreases. Interim analysis shows that T/MWh will continue to decrease at higher power when the condenser vacuum is maintained around the design value.

The performance characteristics of the Turbine-Generator system are expressed in thermal efficiency, which is the ratio of electric power and thermal power as shown in equation (1). The thermal power of the system is calculated by equation (2).

$$\eta_{th} = P_e / P_{th} \quad (1)$$

$$P_{th} = m(h_i - h_o) \quad (2)$$

Where $\mathbf{P_e}$ and $\mathbf{P_{th}}$ respectively, are the electirc and thermal power, **m** is the mass flow rate of the vapor, $\mathbf{h_i}$ and $\mathbf{h_o}$, respectively, are the enthalpy of steam in and out of the turbine. The enthalpy $\mathbf{h_i}$ is determined based on the pressure and temperature of the steam entering the tubine after the strainer, while $\mathbf{h_o}$ is determined based on the vapor pressure out of the turbine with 13% wetness according to the turbine design. Figure 10 shows the relationship between thermal power, thermal efficiency vs. electric power. There is a progressively increasing efficiency when the electric power increases from 0 to 0.6MW. Furthermore, the thermal efficiency is relatively constant at around 55% while the thermal power increases progressively. The low thermal efficiency of the turbine-generator system is most likely due to a pressure loss in the strainer and a significant reduction in the condenser vacuum when electric power is above 0.6MW.

4. CONCLUSION

The 3x24 hour synchronous testing of the 3MW GPP has been successfully implemented. During testing, the steam pressure and temperature entering the turbine are relatively constant around the design value. However, there is a loss of steam pressure entering the turbine by the strainer and reduced condenser vacuum which causes T/MWh from the plant to be still relatively high. All vibration levels are still below the safe limit according to ISO 10816-3 (11.0mm/s for turbines and generators) and according to factory standards (4mm/s for Turbine and Generators, and 8.0 for Gearboxes). The highest bearing temperature is in the generator (around 80ºC) which is probably caused by clearances between the shaft and the bearing that are too narrow. All bearing temperatures are still below the safe limit. The thermal efficiency of the turbine-generator is still around 55%. This can still be improved if the pressure loss in the strainer can be reduced and the decrease in the condenser vacuum can be overcome. The condenser vacuum can be optimized by keeping the cooling water temperature low. From the last inspection, the increase in cooling water temperature was caused by a number of water spray nozzles in the cooling tower that is clogged with dirt. Thus it can be concluded that the plant is ready to operate to full load by improving CT and strainer performance. Until the end of the testing in May 2019, the BPPT GPP has produced 251MWh of electricity, with the highest load of 2.2 MW.

5. ACKNOWLEDGMENTS

The authors would like to thank all directors and managements of Pertamina Geothermal Energy (PGE), for the constant support that contributed to valuable data and the use of field facilities as our research location.

6. REFERENCES

A.S. Karakurt and ÜmitGüneş, J. of Thermal Engineering, Vol. 3, No. 2, pp. 1121-1128 (2017)

BambangTeguh Prasetyo, Suyanto, MAM Oktaufik and Himawan S., Design, Construction and Preliminary Test Operation of BPPT-3MW Condensing Turbine Geothermal Power Plant, EVERGREEN Joint Journal of Novel Carbon Resource Sciences & Green Asia Strategy, Vol. 06, Issue 02, pp.162-167, June 2019

C. T. Hsu, Investigation of an Ejector Heat Pump by Analytical Methods, Prepared by the Oak Ridge National Laboratory, Tennessee 37831, July 1984

CTI, Cooling Tower Institute, Februari 1999.

D. Ion and P.D. Codrut, Efficiency Assessment of Condensing Steam Turbine, Advances in Environment, Ecosystems and Sustainable Tourism, ISBN: 978-1-61804-195-1, 2013, available at http://www.wseas.us/e-library/conferences/2013/Brasov/STAED/STAED-32.pdf

D.K. Bellman et all, Power Plant Efficiency, Working Document of the NPC Global Oil & Gas Study, Made Available July 18, 2007

H. Holmberg, P. Ruohonen and A. Pekka, Determination of the Real Loss of Power for a Condensing and a Backpressure Turbine by Means of Second Law Analysis, Entropy 2009, available at

H. El-Dessouky et all, Evaluation of steam jet ejectors, Chemical Engineering and Processing, 41, (2002) 551–561

HEI Standard: Standards for Direct Contact Barometric and Low Level Condensers, 8th. Ed., 2010

http://adsabs.harvard.edu/abs/2009Entrp..11..702H

J.R. Couper, W.R Penney, J.R. Fair, and S.M. Walas, Chemical Process Equipment – Selection and Design, 2nd. Ed., Elsevier, Oxford, 2010

L. Agustina, S2 Thesis, Program Studi Teknik Panas Bumi - ITB, Bandung, 2013

M. N. Lakhoua, J. of Physical Sciences, Vol. 7(39), pp. 5493-5497, 16 October, 2012, available at http://www.academicjournals.org/IJPS DOI: 10.5897/IJPS12.353 ISSN 1992 -1950 ©2012 Academic Journals.

Mawardi, Economic Optimization of Gas Extraction Systems at Different Levels of Non-Condensable Gas Content, Geothermal Institute, The University of Auckland, 1998

Mechaelidas, The Influence of Non-Condensable Gases on the Net Work Produced by the Geothermal Steam Power Plants, Geothermics, 11, No.3, 163-174 (1982)

M.R. Keith, Maintenance Fundamentals, 2nd. Edition, Elsevier, USA, (2004),

R.H. Perry et all, Perry's Chemical Engineers' Handbook, 7th edition, 1997

ROTALIGN, Ultra Shaft Operating Handbook-Shaft Alignment.

R. DiPippo, Geothermal Power Plants – Principles, Applications and Case Studies, Elsevier, Massachusetts, 2005

R.K. Sinnot, Coulson & Richardson's Chemical Engineering Vol. 6 - Chemical Engineering Design, 4th. Ed., Elsevier, Oxford, 2005

S. Marza, Pengaruh Non-Condensable Gas (NCG) dalam Pemilihan Jenis Sistem Ekstraksi Gas pada Pembangkit Listrik Panas bumi, Institut Teknologi Bandung, Bandung, 2011,.

S. Kakac, Boilers Evaporators & Condensers, John Wiley & Sons, Inc., 1991, p. 613

Suryadarma et.al., "The Kamojang Geothermal Field: 25 Years Operation", in Proceedings World Geothermal Congress 2005, (Antalya, 2005), p. 1

T.C. Elliot, K. Chen and R.C. Swanekamp, Standard Handbook of Powerplant Engineering, 2nd edition, (Mc Graw-Hill, New York, 1989), p. 8.28

T. Surana, Pengembangan Pembangkit Listrik Tenaga Panas Bumi (PLTP) Skala Kecil dan Direct Use, (Final Report, BPPT of Indonesia, Jakarta, 2010)

W. Frohling, H.-M. Unger and Y. Dong, Thermodynamic Assessment Of Plant Efficiencies For HTR Power Conversion Systems, available atwww.iaea.org/inis/collection/NCLCollectionStore/_Public/33/033/33033053.pdf